

## Slow Flip Dynamics in Three-Dimensional Rhombus Tilings: Failure of the Langevin Approach

N. Destainville and V. Desoutter

Laboratoire de Physique Théorique - IRSAMC / CNRS

Université de Toulouse, 31062 Toulouse Cedex, France.

Received September 12, 2007; Accepted November 27, 2007

We study numerically the Markovian flip dynamics in 3D rhombus tilings, a paradigmatic model of quasicrystals. Whereas in 2D, the dynamic is well described by a coarse-grained Langevin approach, its counterpart in 3D fails to account for the observed slow dynamics. We propose a scenario relating this slowing-down to the existence of local obstacles to the movement of tiles, the recently studied “cycles”. Therefore the present system is a novel example where dynamical obstruction is only due to entropic barriers. The non-trivial consequences in terms of both the mechanical properties and the numerical simulation of quasi-crystals are discussed.

**Keywords:** Random tilings, flip dynamics, slow dynamics, Langevin equation.

### 1 Introduction

Random tilings have become a popular topic with the discovery of quasicrystals in 1984 [1, 2]. Penrose tilings and their generalizations rapidly appeared to be suitable paradigmatic models of these quasi-periodic alloys, because their diffraction patterns account for the unusual experimental symmetries (e.g. five-fold axes or icosahedral symmetries). Random tilings are obtained from the quasi-periodic ones by activating some degrees of freedom, the so-called (localized) random flips. The latter are local rearrangements of tiles, which eventually lead to a macroscopic configurational entropy that is supposed to favor quasi-crystals with respect to their quasi-periodic counterparts, while keeping the required symmetries in their diffraction patterns. Quasi-crystals can be in good approximation modeled by decorating tiles with atoms, the idea being that these elementary cells have a relative energetic stability. As compared to usual crystals, there are several unit cells, corresponding to the different tile species that constitute the tiling. Random flips also have their counterpart at the atomic level, called phason flips [3–6]. The study of flip dynamics at the level of tiles is a first, necessary step before focusing on the much more complex

atomic scale. It is the goal of the present Paper. This work follows a previous publications [7] that settled the basics of flip dynamics and tackled the issue of “connectivity by flips”. These former results are summarized below.

There exist several motivations in exploring flip dynamics. First of all, there is a great mathematical interest in studying systems likely to exhibit dynamical obstruction [8, 9], where slow dynamics are not due to any random character of the Hamiltonian, but rather to local geometrical considerations. Structural glasses show a rapid dynamical slowing-down at their glass transition temperature, whereas the interaction potential between its microscopic constituents display no randomness, by contrast to spin glasses. The basic models accounting for glass dynamics appeal to the “cage effect”, where atoms are trapped by their neighbors. Only collective behaviors can unlock these local cages. We shall see that the slow dynamics exhibited in the present work is reminiscent of such an effect.

Beyond this general and mathematical motivation, atomic phason flips are believed to play a notable role in the physical properties of real quasi-crystals. The growth process of quasi-crystals from the liquid phase is not clearly understood (see the review [10]). Atomic interactions can lead only to local interaction rules between tiles, that are unable to propagate the quasi-crystalline order at large distances, whether quasi-crystals at equilibrium are best modeled by perfect quasi-periodic tilings or random ones. Thus the first solidification stage is thought to be followed by a second one involving a large amount of atomic (or tile) rearrangements in order to restore the quasi-periodic order observed at the macroscopic scale. These rearrangements require phason flips, the dynamics of which therefore plays an important role in the growth processes.

Furthermore, self-diffusion is a crucial issue in quasicrystal science, where elementary flips are believed to play an important role because they are a new source of atomic mobility. They could bring their own contribution to self-diffusion [11] in quasi-crystalline alloys, itself being involved in some specific mechanical properties, such as plasticity related to dislocation mobility [7, 12]. Indeed, quasicrystals present a sharp brittle-ductile transition well below their melting transition (for a review, see Ref [13]), which is related to a rapid increase of dislocation mobility [12].

Finally, at the simulation level, Monte Carlo (e.g. [14–19] and the review [20]) or all-atom studies [6] provide quantities that cannot be accessed analytically. They rely on a stochastic sampling of microscopic configurations, itself relying on the assumption that flip dynamics is rapid enough to get sufficiently many independent configurations. However, the issue of sampling rapidity has never been explored in depth so far. In the conclusions of Ref. [7], we evoked the fact that a dynamical slowing-down could arise when focussing on observables different from vertex diffusion. The present work will confirm this point: flip dynamics is slow in sets of random tilings with icosahedral symmetry. Tiles take very long times before finding their equilibrium positions and configurations do not de-correlate rapidly. This result might have non-trivial consequences on the interpretation of both ex-

perimental and numerical data.

## 2 Rhombus Tilings, Generalized Partitions, Cycles

We first present the rhombus tilings under consideration (figures 2.1 (left), 2.2 and 2.3(b)). Then we show how generalized partitions code rhombus tilings. This technique was described into detail in Ref. [7]. We provide a rapid summary. The interested reader will refer to [7], which uses the same notations as the present Paper. The end of the section introduces cycles and flips.

The rhombus random tilings under consideration here are coverings of a region of plane or space by rhombi in 2D and rhombohedra in 3D. They are characterized by the  $D$  possible orientations taken by the edges of the tiles. For example, in two dimensions, such tilings have  $2D$ -fold symmetry (hexagonal for  $D = 3$ , octagonal for  $D = 4$ , etc...). Tilings with icosahedral symmetry in three dimensions correspond to  $D = 6$ .

### 2.1 Rhombus tilings

Rhombus tilings in dimension  $d$  have  $D$  possible edge orientations denoted by  $e_a \in \mathbf{R}^d$ , where  $a = 1, \dots, D$ . Each tiling edge has the orientation and norm of one of the vectors  $e_a$ . A rhombic tile, which is the projection of a  $d$ -cube of  $\mathbf{R}^D$  onto  $\mathbf{R}^d$ , is defined by  $d$  of these edge orientations. The family  $(e_a)_{a=1, \dots, D}$  is supposed to be non-degenerate: any family of  $d$  of its vectors form a basis of  $\mathbf{R}^d$ . This property avoids flat, degenerate tiles. De Bruijn introduced a dual representation of rhombus tilings [21, 22], which consists of seeing the tiling as the dual of a grid of lines (in 2D – see figure 2.3 – or 3D) or surfaces (in 3D, see figure 2.1). This formalism will be quite useful to orient tilings in the following. A de Bruijn line is a sequence (of maximal length) of adjacent tiles that share an edge (in dimension 2) or a face (in dimension 3) with a given orientation. In dimension 3, a de Bruijn surface is a maximal sequence of adjacent tiles sharing an edge with an orientation  $e_a$ . For each orientation  $e_a$ , we denote by  $F_a$  the family of de Bruijn surfaces of a given tiling associated with  $e_a$ . It contains  $p_a$  de Bruijn surfaces, which do not intersect. A tiling with  $D$  orientations of edges living in a  $d$ -dimensional space is called a  $D \rightarrow d$  tiling, and  $D - d$  is its codimension. A tiling is said to be “unitary” if it contains one de Bruijn surface per family ( $p_a = 1$  for all  $a$ ), and “diagonal” if it contains the same number of de Bruijn surfaces in all families ( $p_a = p$  for all  $a$ ). In dimension 3, a rhombic tile is the intersection of three surfaces of different families and there are  $\binom{D}{3}$  different species of tiles. Finally, we denote by  $\mathcal{T}((e_a), (p_a))$  (or by  $\mathcal{T}$  for short) the set of tilings with edge orientations  $(e_a)_a$  and with  $p_a$  de Bruijn surfaces in family  $F_a$ .

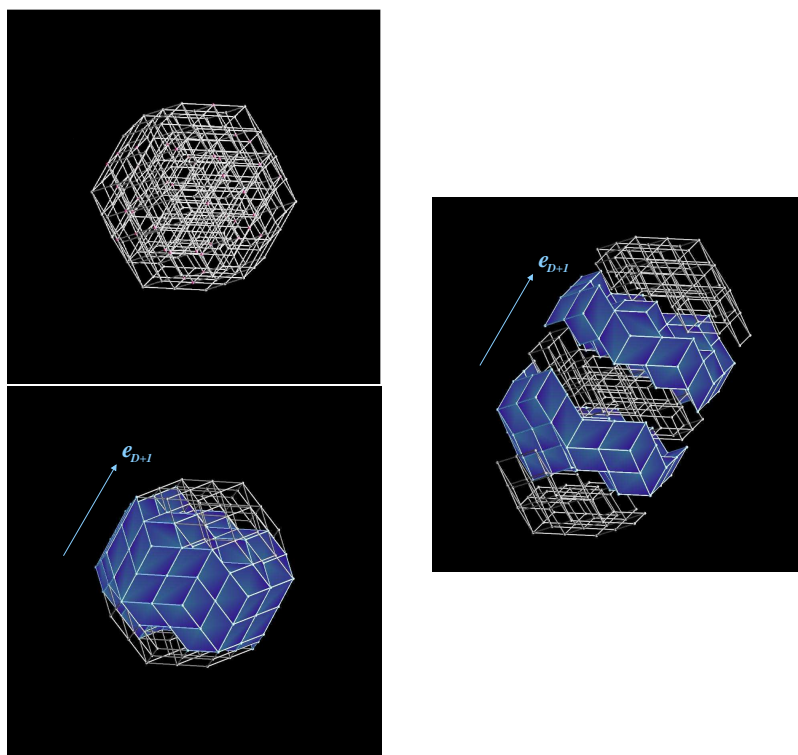


Figure 2.1: Three different representations of a same diagonal  $6 \rightarrow 3$  tiling with icosahedral symmetry and  $p = 2$ , filling a triacontahedron. Left, top: “stick and ball” representation; bottom: the two de Bruijn surfaces of the sixth family  $F_6$  are represented in blue. Right: Exploded view. The de Bruijn surfaces of  $F_6$  are still in blue, whereas the remaining tiles are transparent. The base tiling associated with the leading vector  $e_{D+1} = e_6$  is composed of these latter tiles when the blue ones are removed. The three domains  $\mathcal{D}_0$ ,  $\mathcal{D}_1$  and  $\mathcal{D}_2$  are clearly identifiable, from bottom to top.

## 2.2 Flips Markovian dynamics and connectivity

Rhombus tilings possess specific local degrees of freedom that are called elementary flips or localized phasons. In dimension  $d$ , a flip consists of a local rearrangement of  $d + 1$  tiles filling a small polytope embedded in a tiling. In dimension 2, it is a rearrangement of 3 tiles inside an hexagon, and in dimension 3, of 4 tiles inside a rhombic dodecahedron, as illustrated in Figure 2.2.

Giving access to a large amount of microscopic configurations, these random flips are the source of a finite configurational entropy,  $\sigma$ , depending, among several parameters, on  $d$  and  $D$ , on the integers  $p_a$ , and on boundary conditions (see below) [20].

A question naturally arises at this stage: is  $\mathcal{T}((e_a), (p_a))$  connected by flips? In other

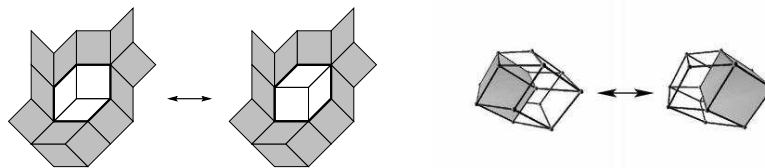


Figure 2.2: Examples of flips: Left: a 2-dimensional flip inside an hexagon involves 3 tiles (and 3 edge orientations). Right: a 3-dimensional flip inside a rhombic dodecahedron involves 4 tiles (and 4 edge orientations). For sake of clarity, the surrounding tiling has not been represented.

words, given any two tilings  $t_1, t_2 \in \mathcal{T}((e_a), (p_a))$ , is it possible to find a finite sequence of flips that goes from  $t_1$  to  $t_2$ ? This issue has been tackled in Ref. [7]. We shall give below the principal conclusions of this study. In general, the answer is positive.

Flips also enable one to define a Monte Carlo Markovian dynamics on tiling sets as follows (see e.g. [7] and references therein for additional details): choose randomly a vertex with uniform probability  $1/N_V$ ,  $N_V$  being the number of vertices. If this vertex is flippable (it is surrounded by  $d + 1$  tiles in dimension  $d$ ), then flip it. In the following, the time unit will be the Monte Carlo Sweep (MCS). It corresponds to  $N_V$  attempted flips. This Markovian process satisfies the detailed balance condition and converges towards the uniform distribution on  $\mathcal{T}$ , provided  $\mathcal{T}$  is connected by flips. This Markovian dynamics has been mainly studied in dimension 2. It has been demonstrated that it is rapid in codimensions 1 [23] and 2 [24]. This means that the typical time to reach equilibrium is polynomial in the number of tiles (the system size). The same conclusion holds in the  $4 \rightarrow 3$  case, as it has been established numerically [25]. In contrast, this question remains open in dimension  $d = 3$  for  $D \geq 5$  and it is our purpose to tackle it, which will be done in Sections 3 and 4.

### 2.3 Edge orientations, boundaries and coarse-graining

So far, we have used families of edge orientations,  $(e_a)_{a=1, \dots, D}$ , without discussing the role of the relative positions of the vectors  $e_a$ . It is clear that a small rotation of one or several of these vectors will change the tiling geometry but not its topology. How far can the family  $(e_a)$  be deformed without affecting tiling topology? This question has been answered in Ref. [7] as follows: depending on  $D$ , there can exist several topological equivalence classes, each class containing edge orientations which define topologically equivalent tiling sets. For  $d = 2$ , or  $d = 3$  and  $D \leq 5$ , or  $D - d \leq 2$ , there is a unique class. For  $d = 3$  and  $D = 6$  (resp.  $D = 7$ ), there are 4 (resp. 11) classes. This classification relies on a mapping of  $\mathbf{R}^3$  onto the projective plane  $\mathbf{PR}^2$ . It can be in principle extended to any  $d$  and  $D$ .

Setting these edge orientations also prescribes the tiling boundaries. Indeed, the generalized partition method that we use in this Paper imposes fixed boundaries to the tilings.

These boundaries are not necessarily regular polytopes (see Ref. [26]), but the formalism is much easier in this latter case. These polytopes are more precisely zonotopes, the projections of  $D$ -dimensional rectangular parallelotopes onto  $\mathbf{R}^d$  (examples given in figures 2.1 and 2.3). There are 4 (resp. 11) such topologically different zonohedra for  $D = 6$  (resp. 7). For  $d = 2$ , there is only one zonogone, the centro-symmetric  $2D$ -gon of sides  $p_1, \dots, p_D$  [7]. Note that with such boundaries, the dual de Bruijn grids are “complete”, that is to say that any de Bruijn line (resp. surface) in 2D (resp. 3D) intersects any de Bruijn line (resp. surface) of another family. This property simplifies greatly tiling manipulations at the numerical level.

These polyhedral boundary conditions are known to have macroscopic effects on random tilings [26]. In the thermodynamic limit of large system size, the statistical ensemble is dominated by tilings that are fully random only inside a finite fraction of the tiling and are frozen in macroscopic domains near the boundary. By frozen, we mean that they exhibit simple periodic tilings, with a zero contribution to the configurational entropy. Therefore fixed-boundary tilings have a lower entropy per tile as compared to free- or periodic-boundary ones. In two dimensions, this is known as the “arctic circle phenomenon” (see e.g. Ref [26] and references therein). Such fixed-boundary conditions are not physical, by contrast to free ones (see the discussion in Ref. [26]). Thus several studies have related fixed boundary conditions to free ones, and have shown that there exists an exact, formal relation between the corresponding entropies [28]. A quantitative relation has even been calculated in the  $3 \rightarrow 2$  case [27,28], but it has not been possible so far to extend it to more general categories of tilings except by numerical means [25,26], because establishing this relationship requires the analytical knowledge of the free-boundary entropy.

To explain how different boundary conditions are related, we need introducing some additional concepts. Because rhombic or rhombohedral tiles are the projection of  $d$ -dimensional faces of  $D$ -dimensional hyper-cubes, a tiling can be represented as a  $d$ -dimensional directed hypersurface embedded in a  $D$ -dimensional Euclidean space. For example, when  $d = 2$  and  $D = 3$ , this hypersurface consists of the faces of the stacking of cubes viewed from the (1,1,1) direction of the 3-dimensional cubic lattice (figure 2.3(a)). When projected along the same direction on the “real” space  $\mathbf{R}^2$ , it becomes a plane tiling. It is said to be “directed” because no tile overlaps occur during the projection. The same relationship holds for  $d = 3$  and  $D = 4$ : the directed hyper-surface consists now of the 3-dimensional faces of the stacking of 4-dimensional hypercubes viewed from the (1,1,1,1) direction. Since the hyper-surface is directed, it can be seen as a mono-valued, continuous, piecewise linear function  $\phi$  from the real space  $\mathbf{R}^3$  to  $\mathbf{R}$ . The value of  $\phi$  is just the height along the (1,1,1,1) axis in this case. This point of view can be easily extended to larger values of  $D$ , where  $\phi$  is now defined on  $\mathbf{R}^d$  and takes its values in  $\mathbf{R}^{D-d}$ .

In the thermodynamic limit, these piecewise linear functions  $\phi$  can be coarse-grained to obtain smooth functions  $\varphi : \mathbf{R}^d \rightarrow \mathbf{R}^{D-d}$  which only contain the large wavelength

fluctuations of the original corrugated membranes  $\phi$  [20]. The tiling entropy is now contained in short wavelength fluctuations of the associated hyper-surface  $\varphi$ . They play the role of macroscopic states in a statistical physics point of view. Small-scale fluctuations are integrated in an entropy functional,  $s[\varphi]$ , that is proportional to the logarithm of the total number of possible piecewise linear hyper-surfaces  $\phi$  that are close to the smooth one  $\varphi$ . The function  $\varphi_{\max}$  that maximizes  $s[\varphi]$  represents the dominant macroscopic state of the system. Note that  $s[\phi]$  can always be written as a functional of the gradients of  $\phi$ . The latter are known as the “phason gradients” in quasi-crystallography.

Fixed boundaries on tilings translate into fixed boundary conditions for the functions  $\phi$  or  $\varphi$ . Therefore  $s[\varphi]$  must be maximized on a restricted set of functions having these boundary conditions, denoted by  $\Phi$ . For  $d = 3$ , the boundaries of functions  $\varphi \in \Phi$  are non-flat polyhedra, and the phason gradient of  $\varphi$  cannot vanish everywhere. Therefore their entropy per tile satisfies  $\sigma_{\text{fixed}} < \sigma_{\text{free}}$ , as anticipated above. Coming back to the frozen regions discussed previously, they result from the fact that  $\varphi_{\max}$  is affine on macroscopic regions near the boundary, and that its phason gradient corresponds there to periodic tilings. For  $d = 2$  and  $D = 3$ , it has been proven that, at the large size limit, the frontier between the frozen and unfrozen regions is a perfect circle, the so-called “arctic circle” [27]. For  $d = 3$  tilings with polyhedral boundaries, it has been conjectured numerically that this arctic frontier is also polyhedral because the entropic repulsion between de Bruijn surfaces is weak and short-ranged, in contrast to  $d = 2$  [25, 26]. A consequence of this conjecture is that, in three dimensions, there exists a macroscopic inner region,  $\mathcal{R}_{\text{free}}$ , where the tilings have completely forgotten their fixed boundaries and are strictly speaking equivalent to free-boundary ones. In addition, this region  $\mathcal{R}_{\text{free}}$  is the sole region that is effectively of type  $D \rightarrow d$ . Surrounding regions have a lower effective codimension because they do contain a subset of all the available edge orientations only. We shall use this result below.

## 2.4 Generalized partitions

An alternative description of the same tilings appeals to generalized partitions which are a re-phrasing of the corrugated functions  $\phi$ . The idea is an iterative construction, where the dual grid is coded with the help of integers satisfying suitably defined partial order relations. In dimension 3, one begins with a complete grid made of three families of surfaces, which represents a  $3 \rightarrow 3$  periodic tiling with one type of tiles. In order to build a  $4 \rightarrow 3$  tiling, one has to prescribe where to place the de Bruijn surfaces of the fourth family  $F_4$ , relatively to the existing intersections of 3 surfaces. Beyond  $F_4$ , if one wants to build a  $D + 1 \rightarrow 3$  tiling, denoted by  $t$ , starting from a  $D \rightarrow 3$  one (called the “base” tiling and denoted by  $T_b$ ), one has to describe where to place the family  $F_{D+1}$  of surfaces. To be sure to obtain a tiling by this process, some constraints must be imposed on the way to place the family  $F_{D+1}$ . First of all, the surfaces of this family must not intersect. In addition, no more

than 3 surfaces can cross at the same point, otherwise some tiles are not properly defined. Furthermore, de Bruijn surfaces are themselves “directed”. It means that they can also be seen as mono-valued functions  $\mathbf{R}^2 \rightarrow \mathbf{R}$  defined on a (2D) plane normal to their orientation vector  $e_a$ .

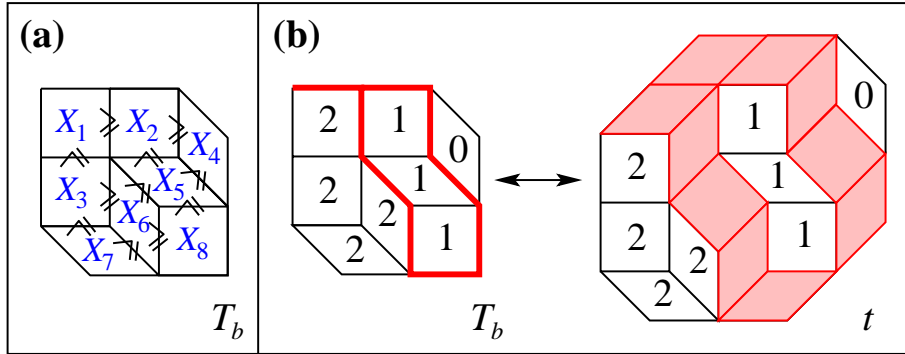


Figure 2.3: Illustration of the the generalized partition technique in 2 dimensions: Construction of a  $4 \rightarrow 2$  tiling,  $t$ . (a): Order relation between the parts  $X_1, \dots, X_8$  of the 8-tile base  $3 \rightarrow 2$  tiling,  $T_b$ ; (b): One solution of this generalized partition problem codes bijectively a  $4 \rightarrow 2$  tiling. The de Bruijn family  $F_4$  contains two lines. Their tiles are colored, whereas the remaining white ones belong to the base tiling  $T_b$ . The domains  $\mathcal{D}_0$ ,  $\mathcal{D}_1$  and  $\mathcal{D}_2$  appear as the tiles bearing parts equal to 0, 1 and 2, respectively. They are separated by the two de Bruijn lines of  $F_4$ .

These considerations enable one to define a partial order relation between the tiles of  $T_b$ , in order to satisfy these constraints, as follows (see also two illustrations in figures 2.1 and 2.3). Since the  $p_{D+1}$  de Bruijn surfaces of the family  $F_{D+1}$  of  $t$  do not intersect, they divide the space  $\mathbf{R}^d$  into  $p_{D+1} + 1$  disjoint domains. Furthermore, since de Bruijn surfaces are all oriented, we can index these domains from 0 to  $p_{D+1}$  so that, following the direction given by  $e_{D+1}$ , we go through all these domains in an increasing order. They are denoted by  $\mathcal{D}_0, \dots, \mathcal{D}_{p_{D+1}}$  and the surfaces of  $F_{D+1}$  by  $S_1, \dots, S_{p_{D+1}}$ . The de Bruijn surface  $S_k$  lies between the domains  $\mathcal{D}_{k-1}$  and  $\mathcal{D}_k$ . In other words, the tiles of  $t$  that do not belong to the surfaces of  $F_{D+1}$  belong to one of the domains  $\mathcal{D}_k$ . Now we contract (or delete) the tiles of  $F_{D+1}$  from  $t$ , for example by setting the length of  $e_{D+1}$  to 0. This gives a  $D \rightarrow d$  tiling,  $T_b$ . Two adjacent tiles of  $T_b$ , with one above the other along the direction given by  $e_{D+1}$ , either belong to the same domain  $\mathcal{D}_k$ , or are separated by one (or several) de Bruijn surface of  $F_{D+1}$ , the tile atop being in the higher domain. This remark leads naturally to the definition of an order relation,  $\leq_{D+1}$ , relatively to  $F_{D+1}$ , between the tiles of  $T_b$ . Let  $u$  and  $v$  be any two adjacent tiles of  $T_b$ ,  $u \leq_{D+1} v$  means that  $u$  is below  $v$  along  $e_{D+1}$ . This order relation is only partial [7].

Now we return to our initial goal which was to code the position of the de Bruijn



surfaces of  $F_{D+1}$  on the  $D \rightarrow 3$  base tiling  $T_b$ . We proceed by associating an integer  $X_u$ ,  $0 \leq X_u \leq p_{D+1}$ , to each tile  $u$  of  $T_b$ :  $X_u$  will be equal to the index  $k$  of the domain  $\mathcal{D}_k$  to which  $u$  belongs. These integers (or by extension the variables  $X_u$ ) are called “parts”. They are constrained by the partial relation order  $\leq_{D+1}$  (which for convenience we shall simply denote by  $\leq$  from now). A “generalized partition”  $(X_u)_{u \in T_b}$  on  $T_b$  is a collection of integers satisfying these two-conditions: (i)  $0 \leq X_u \leq p_{D+1}$  and (ii) for any two tiles  $u$  and  $v$ , if  $u \leq v$ , then  $X_u \leq X_v$ . By construction, the set of all the possible  $D + 1 \rightarrow 3$  tilings  $t$  generated from  $T_b$ , is in bijection with the set of partitions  $(X_u)$ . In figure 2.3, one can see an example of a  $4 \rightarrow 2$  tiling coded by a generalized partition on a  $3 \rightarrow 2$  tiling.

To sum up, we have established a one-to-one correspondence between  $D + 1 \rightarrow 3$  tilings and pairs composed of (i) a base  $D \rightarrow 3$  tiling and (ii) a generalized partition on this base tiling. This one-to-one coding of zonotopal tilings is described in a more formal way in reference [29]. By induction on  $D$ , it enables one to code  $D \rightarrow 3$  tilings, starting from the simplest case of partitions on  $3 \rightarrow 3$  tilings. The latter can be seen as 3-dimensional rectangular arrays where parts are decreasing in each row, line, and column. These partition problems are usually called solid partition problems [29]. Let us remark that when one codes  $D + 1 \rightarrow 3$  tilings by this generalized partition technique, the order in which the de Bruijn families of surfaces are successively added to the tilings is arbitrary. At the last step of this process, one is for example free to choose the  $D$  edge orientations defining the base tilings among the  $D + 1$  possible ones, or equivalently one  $e_a$  among the  $D + 1$  possible ones to define the order relation  $\leq$ . This particularized vector  $e_a$  is called the “leading edge orientation”. Unless expressly specified, this leading vector is supposed to be  $e_{D+1}$ .

## 2.5 Cycles

Now we introduce the notion of “cycle” on a base tiling [7] that will play an important role in the following. A cycle is a sequence of pairwise adjacent tiles,  $\Gamma = (u_1, u_2, \dots, u_n, u_1)$ , such that:  $X_{u_1} \leq X_{u_2} \leq \dots \leq X_{u_n} \leq X_{u_1}$ , with respect to the previous partial order relation. Note that the first and last tiles coincide, which implies that the tiles inside the cycle have to be equal to a unique part:  $X_{u_1} = X_{u_2} = \dots = X_{u_n} = X_0$ . Geometrically speaking, a cycle is a sequence of tiles making a “loop” such that each tile is placed below the next one relatively to the orientation prescribed by  $e_{D+1}$ . Thus a de Bruijn surface of family  $F_{D+1}$  is either completely above or completely below a cycle, which is indeed equivalent to say that the cycle tiles must bear equal parts. A base tiling containing at least one cycle is said to be “cyclic”, while a tiling without any cycle is “acyclic”. Such cycles have been studied into detail in Ref. [7], where a commented example is given. It has been demonstrated that, far from being exceptional, cycles are generic in 3D tilings as soon as  $D \geq 6$ . For  $D = 4$  and  $D = 5$ , as well as for  $d = 2$  and any  $D$ , tilings are always acyclic. Furthermore, nothing prevents *a priori* the occurrence of several independent

cycles in a same base tiling (possibly bearing different parts).

In Section 2.3 above, we have explained that for a given  $D$  and  $d$ , there can exist several non-equivalent classes of edge orientations  $(e_a)_a$ . It turns out that all classes are not on an equal footing as far as the existence of cycles is concerned. In Ref. [7], it has been proven that in general, there exists at least one  $a$  such that, if  $e_a$  is the leading vector (see Section 2.4), all base tilings are acyclic. It was also demonstrated that this property implies connectivity by flips of tiling sets. But there also exist some classes of edge orientations for which *it cannot be proven* that there exists such a leading vector  $e_a$ . Consequently, in these rare cases, connectivity cannot be proved with the technique developed in Ref. [7]. It does not mean that connectivity is broken but simply that this question remains open. There is one such class for  $D = 6$  (among 4 classes) and 2 classes among 11 for  $D = 7$ . For  $D = 6$ , this class appears to correspond to the icosahedral symmetry of physical interest. The 3 remaining classes do not correspond to any physical, quasi-crystalline symmetry. Furthermore, they do not exhibit any cycle, whatever the leading vector  $e_a$ ,  $a = 1, \dots, 6$ . This dichotomy between classes for which connectivity is established, and those for which it remains open, will play a notable role below.

To close this section, we mention that V. Desoutter has proven the following important result [30]: let  $T_b$  be any base tiling. Let us denote by  $\mathcal{F}(T_b)$  the subset of  $\mathcal{T}$  containing all the tilings, the base tiling of which is equal to  $T_b$ . Then whatever  $d$  and  $D$ , whatever the class of edge orientations  $(e_a)_a$ , and whatever the leading vector  $e_a$  chosen to define the order relation  $\leq$ , there always exist at least one base tiling,  $T_b$ , such that  $\mathcal{F}(T_b)$  is connected by type-II flips. We shall not reproduce the proof of this result here because it would require to introduce additional definitions and lemmas.

## 2.6 Flips in the generalized partition formalism

What do flips become in the generalized partition point of view? In a generalized partition problem on a  $D \rightarrow d$  tiling (which codes  $D + 1 \rightarrow d$  tilings), one distinguishes two types of flips [7]. Type-I flips involve only tiles of the base  $D \rightarrow d$  tiling and no tile of the de Bruijn family  $F_{D+1}$ . As a consequence, the  $d + 1$  tiles bear equal parts and belong to a same domain  $\mathcal{D}_k$ . Flipping these tiles only changes the base tiling without modifying the parts attached to the flipped tiles. Type-II flips involve tiles that belong to the de Bruijn family  $F_{D+1}$ . More precisely, they involve  $d$  tiles having an edge parallel to  $e_{D+1}$ , belonging to a same surface  $s_0$  of the family  $F_{D+1}$ , and only one tile,  $u_0$ , in the base tiling. When flipping these tiles, the position of  $s_0$  relatively to  $u_0$  is modified. If  $u_0$  lied below (resp. above)  $s_0$  before the flip, it goes above (resp. below)  $s_0$  afterwards. Thus the flip changes the part  $X_{u_0}$  borne by  $u_0$  by  $\pm 1$ .

Now we recall that a cycle  $\Gamma$  in a tiling is a closed sequence of pairwise adjacent tiles, which are constrained to bear the same part in the generalized partition problem. Conse-

quently, the tiles of  $\Gamma$  cannot participate to any type-II flip, since we have just seen that it would change the part of a single tile, to a value different from that of the whole cycle. Geometrically speaking, a de Bruijn surface  $s_0$  of  $F_{D+1}$  cannot pass through a cycle. It is constrained to be either completely above or completely below the cycle. If  $s_0$  is initially below (resp. above) the cycle  $\Gamma$ , one must first break  $\Gamma$  by type-I flips, if it is possible, so that  $s_0$  can jump above (resp. below)  $\Gamma$ . We say that the tiling is locally jammed to emphasize that some geometric obstacles must be “healed” to allow the free movement of de Bruijn surfaces.

### 3 A Survey of the Langevin Approach of Flip Dynamics

Owing to the previous considerations, it is reasonable to anticipate that cycles might have an influence on the Markovian flip dynamics. Forbidding some type-II flips, they reduce locally the degrees of freedom related to those flips because of jammed clusters of tiles. They are susceptible to slow down the dynamics, in the sense of an increase of ergodic times. In Ref [7], this issue was first addressed by studying the diffusion of vertices *via* flip dynamics. Numerical evidences suggested that diffusion was not notably slowed down by cycles.

The standard approach to flip dynamics appeals to an approximate Langevin approach [31] using the coarse-grained entropy (or free-energy) functional  $s[\varphi]$ , which is usually well suited to describe Markovian dynamics in configuration sets at the thermodynamic limit. Quoting L.J. Shaw, V. Elser and C.L. Henley, “The linear-response dynamics can always be described by an equation of [this] form” [15]. The idea is formalized as follows: the coarse-grained functional,  $s[\varphi]$ , can be written, in the small gradient approximation, in a quadratic form:  $s[\varphi] = s[\varphi_{\max}] - \frac{1}{2} \int_V \sum_{i,j} \nabla \varphi_i(\mathbf{r}) \cdot \mathbf{K}_{ij} \cdot \nabla \varphi_j(\mathbf{r}) \, d^2\mathbf{r}$ , where  $\mathbf{K}$  is the tensor of phason elastic constants, and the  $\varphi_i$  are the coordinates of  $\varphi$  in  $\mathbf{R}^{D-d}$ . In the Fourier space, this expression becomes [15]:

$$s[\hat{\varphi}] = s[\varphi_{\max}] - \frac{1}{2} \sum_{\mathbf{q}} \sum_{i,j} \hat{\varphi}_i(\mathbf{q}) \cdot \mathbf{K}_{ij}(\mathbf{q}) \cdot \hat{\varphi}_j(\mathbf{q}). \quad (3.1)$$

The Langevin formalism prescribes the evolution of  $\hat{\varphi}_i(\mathbf{p}, t)$  [15]:

$$\frac{d\hat{\varphi}_i(\mathbf{q})}{dt} = - \sum_j \Gamma_{ij}(\mathbf{p}) \frac{\delta s[\hat{\varphi}]}{\delta \hat{\varphi}_i(\mathbf{q})} + \zeta_i(\mathbf{q}, t), \quad (3.2)$$

where  $\zeta$  is a stochastic noise and  $\Gamma_{ij}(\mathbf{p})$  are the dissipation constants. They are quadratic in  $\mathbf{p}$  because of the gradients in  $s[\varphi]$ . This equation means that the system follows the entropy gradients in the configuration set  $\mathcal{T}$  and is also subject to the thermal noise  $\zeta$ . Numerically, the latter is mimicked by the randomness of the Monte Carlo elementary moves. Inserting the quadratic form (3.1) in the Langevin equation (3.2), one gets a linear differential system,

which can be tackled by usual tools of algebra and analysis. It is then found [15] that the slowest, small  $\mathbf{q}$  (or equivalently long wave-length) modes decay exponentially with time with a characteristic time proportional to  $1/\mathbf{q}^2$ .

To sum up, this approach predicts that our finite systems of linear size  $L \propto p$  relax to equilibrium with a time scale proportional to  $p^2$ :

$$\tau_{\text{corr}} \propto p^2. \quad (3.3)$$

We recall that  $p$  is the number of de Bruijn surfaces per family in diagonal tilings.

While it has been demonstrated in two dimensions that characteristic time-scales to reach equilibrium are indeed of this form [24], the question remains open in three dimensions. The only numerical studies available so far, concerning  $4 \rightarrow 3$  tilings [25] and icosahedral ones [15], were consistent with Eq. (3.3). However, the Langevin approximation assumes that the slowest modes are the long-wavelength ones, which justifies the coarse-grained form of the entropy functional used above. Even if short-wavelength physics are hidden in  $s[\phi]$ , they are implicitly supposed not to affect the correlation time  $\tau_{\text{corr}}$ , because it is dominated by long wavelengths.

In order to track any sign of slow dynamics at short wave-lengths, an approach consists of studying vertex diffusion. Indeed, it has been demonstrated that tile vertices can travel long distances across the tiling by flip activation [11]. Assuming a diffusion coefficient,  $\kappa$ , independent of the tiling size  $p$ , the typical diffusion time to explore the whole tiling is  $\tau_{\text{diff}} \sim L^2/\kappa \propto p^2 \propto \tau_{\text{corr}}$ . It is indeed what was observed numerically, together with a  $\kappa$  independent of  $p$  [7, 32]. Again, these findings are consistent with the Langevin approximation. In these diffusion numerical experiments, the only manifestation of small-wavelength dynamics was a short-time anomalous diffusion attributed to flip correlations: A flip has a significant chance to be followed by the reverse one.

## 4 Numerical Study of Flip Dynamics in Dimension 3

In order to analyze further the possible effect on ergodicity of cycles on flip dynamics, we now characterize the temporal evolution *via* a different observable, namely the mean part value. This observable is not directly related to the diffusion of vertices but to that of tiles and de Bruijn surfaces. While vertices diffuse over long distances in tilings, geometric constraints prevent tiles from traveling long distances [11], because each de Bruijn surface of a family is constrained by the closeness of its two neighbors of the same family. We have also discussed that cycles are strong obstacles to the movement of these surfaces, and therefore to the movement of tiles attached to them. But tile positions in the tiling are coded by parts in the generalized partition formalism. Thus it is legitimate to anticipate that if ergodicity is broken because of cycles, part dynamics will be affected. That is why we measure tile positions with the help of part values. Here we focus on parts relative to a

given order relation  $\leq_a$  among the  $D + 1$  possible ones, keeping in mind that it is a partial information on tile positions. However, we shall see that this observable is sufficient to demonstrate the existence of slow dynamics.

Thus we track the mean part value as a function of time for a given leading vector  $e_a$ . That is to say, for a tiling  $T$  of type  $D + 1 \rightarrow d$  and of base tiling  $T_b$ , we average the parts  $X_u$  of the generalized partition on  $T_b$ . This mean value at time  $t$  is

$$\Psi_{(a,T)}(t) = \frac{1}{N(T_b)} \sum_u X_u, \quad (4.1)$$

where  $N(T_b)$  is the number of tiles of  $T_b$ . The interest of this quantity is that we know in advance its equilibrium value. Thus it will be easy to know if tilings have returned to equilibrium at a given time. More precisely, at equilibrium, for a tiling the parts of which are comprised between 0 and  $p_a$ , one has:

$$\langle \Psi_{(a,T)}(t) \rangle = \frac{p_a}{2}, \quad (4.2)$$

where the average is over realizations. Indeed, generalized partitions are symmetrical with respect to the value  $p_a/2$  because, given any tiling  $T$  with  $\Psi_{(a,T)} = \bar{X}$ , there exists a symmetrical tiling,  $T'$ , for which  $\Psi_{(a,T')} = p_a - \bar{X}$ :  $T'$  is the symmetrical of  $T$  with respect to the center of the boundary zonotope (a zonotope is always centro-symmetrical). For sake of simplicity, we focus here on so-called ‘‘diagonal’’ tilings, where  $p_a = p$  for any  $a$ . To study the time-evolution of  $\Psi_{(a,T)}(t)$  by Monte Carlo flip dynamics, we first prepare an initial tiling,  $T_0$ , with  $\Psi(t = 0) = 0$ , by first constructing a  $D \rightarrow d$  base tiling,  $T_b$ , then the  $D + 1 \rightarrow d$  tiling,  $T_0$ , by setting all the parts to 0 on  $T_b$ .

Now we focus on  $6 \rightarrow 3$  tilings, of physical interest, the base tilings of which are of type  $5 \rightarrow 3$ . Conclusions are strictly similar for  $7 \rightarrow 3$  ones (data not shown [30]). We can already notice that the possible effects of cycles were not observable up to  $p \simeq 15$  for icosahedral tilings. For smaller sizes, cycles are not manifestly abundant enough to slow down dynamics [7]. Note that it is already impossible, for such sizes, to test directly whether base tilings are cyclic or not, because the complexity of cycle-search algorithms grows rapidly with  $p$  [30].

We display, in Figure 4.1, the evolution of  $\Psi_{(a,T)}(t)$  for two unique  $6 \rightarrow 3$  tilings representative of the cyclic and acyclic cases, with  $p = 10$  and  $p = 20$ . One can see in this figure a sticking difference between tilings *a priori* containing cycles and acyclic ones when  $p = 20$ . For the latter,  $\Psi_{(a,T)}(t)$  evolves rapidly towards its equilibrium value,  $p/2$ , with an equilibration time, equal to  $\tau_{\text{corr}}$ , of order  $2 \cdot 10^4$  MCS. Then it fluctuates around  $p/2$ . In addition, the observed equilibrium times are entirely compatible with the  $p^2$  behavior predicted by the previous Langevin approach.

By contrast, in the case of icosahedral cyclic tilings,  $\Psi_{(a,T)}(t)$  grows rapidly, with the same characteristic time, towards a value lower than  $p/2$  before fluctuating around it, thus

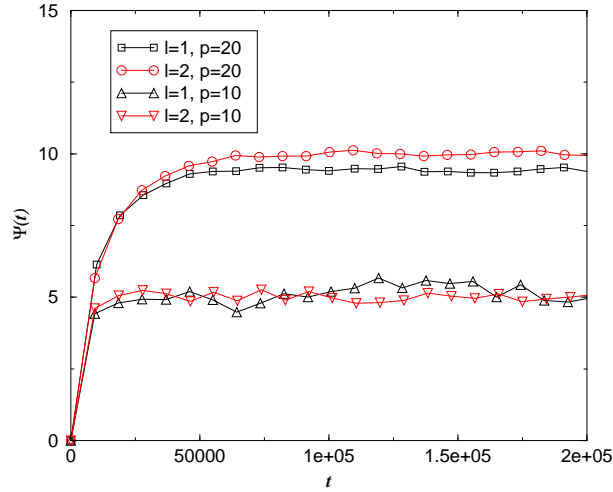


Figure 4.1: Temporal evolution of the mean part value for  $6 \rightarrow 3$  tilings. We have represented the evolution of a tiling with icosahedral symmetry ( $l = 1$ ), likely to contain cycles, and of a tiling belonging to the second 6-line arrangement ( $l = 2$ ). We know that the second one is acyclic. For  $p = 10$ , one can see that, after a short transient,  $\Psi_{(a,T)}(t)$  fluctuates around its equilibrium value,  $p/2$ , in both cases. By contrast, for  $p = 20$ , while acyclic tilings return rapidly to equilibrium, their icosahedral counterpart seems to be pinned at a value strictly lower than  $p/2$ . Times are in MCS units.

revealing an out-of-equilibrium state. In order to exclude that this observations might be simply due to large fluctuations around  $p/2$ , we have computed the evolution averaged over 10 realizations, as shown in figure 4.2. One can see that  $\Psi_{(a,T)}(t)$  is pinned below its equilibrium value,  $p/2$ . No return at equilibrium has been observed for simulation times up to  $10^6$  MCS. This is the manifestation of an ergodicity breaking in flip dynamics for icosahedral tilings.

For  $7 \rightarrow 3$ , tilings, our conclusions are similar [30], with the complication that there exist edge orientations for which tilings are acyclic for only a few choices of the leading vector  $e_a$ . In this case, we have shown that  $\Psi_{(a,T)}(t)$  returns rapidly to  $p/2$  for any  $a$ , with a higher equilibration time of order  $10^5$ . Thus the slowing-down revealed by our simulations occurs only when there exist cycles for *all* leading vectors  $e_a$ . In this  $D = 7$  case, this slowing-down, when it exists, is already visible at  $p = 10$ . For this tiling size, we have observed rare returns at equilibrium. Even though it is strongly realization-dependent, we have found a numerically accessible characteristic time for a few realizations, around  $7 \cdot 10^5$  MCS.

In addition, this slowing-down cannot be due to a possible connectivity breaking of the configuration set and is necessarily related to the existence of some entropic barriers: in the

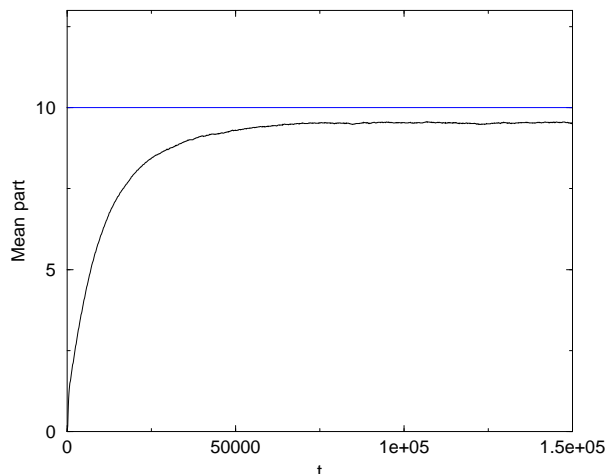


Figure 4.2: Evolution of the mean part averaged over 10 icosahedral tilings. In the stationary regime, there is a deviation from the expected value  $p/2$  that cannot be attributed to fluctuations of  $\Psi_{(a,T)}(t)$ . Even if the system eventually returns to equilibrium, characteristic times will be much higher than in the acyclic cases. Times are in MCS units.

present problem, there is no energy and therefore no energy barrier. Indeed, we are going to demonstrate that, even if the configuration set were not connected by flips – which remains an open issue –, the connected component of the initial tiling  $T_0$  where the dynamics occurs, denoted by  $\mathcal{C}(T_0)$ , is symmetrical with respect to the value  $p/2$ . This implies that the equilibrium value of  $\Psi$  is equal to  $p/2$  in  $\mathcal{C}(T_0)$ . Remind that  $T_0$  had all its parts equal (to 0) on its base tiling. In such a tiling  $T_0$ , all type-I flips are possible. In particular, given any tiling  $T \in \mathcal{C}(T_0)$ , its centro-symmetrical tiling,  $T'$ , is always accessible by flips as follows: one first returns to the initial tiling,  $T_0$ ; then one can have access, by type-I flips, to a base tiling  $T_b$  such that  $\mathcal{F}(T_b)$  is connected by type-II flips (such a  $T_b$  exists, see Section 2.4). Then all the parts are set to their maximal value  $p$  by type-II flips. One has thus reached the centro-symmetrical tiling of  $T_0$ , denoted by  $T'_0$ . Now one executes the sequence of flips that is centro-symmetrical of the preceding one and arrives at  $T'$ , while staying in  $\mathcal{C}(T_0)$ . Therefore  $T' \in \mathcal{C}(T_0)$  and  $\Psi_{(a,T')} = p - \Psi_{(a,T)}$ .

In order to better characterize these slow dynamics, we have also analyzed how part values are distributed. More precisely, each tile  $u$  of the base tiling is tracked during the time evolution. The part  $X_u$  that it bears is recorded and it is averaged over a time interval, chosen to be equal to  $2 \cdot 10^4$  MCS in the present case. This average is denoted by  $\langle X_u \rangle$ . The so-obtained parts distributions are expected to be symmetrical with respect to  $p/2$  once equilibrium has been reached. We display in figure 4.3 two typical examples for  $6 \rightarrow 3$  tilings. The first one corresponds to a class of edge orientations for which we know that all

base tilings are acyclic. It is measured once equilibrium has been reached; The second one is measured in the icosahedral case when stationarity has been reached.

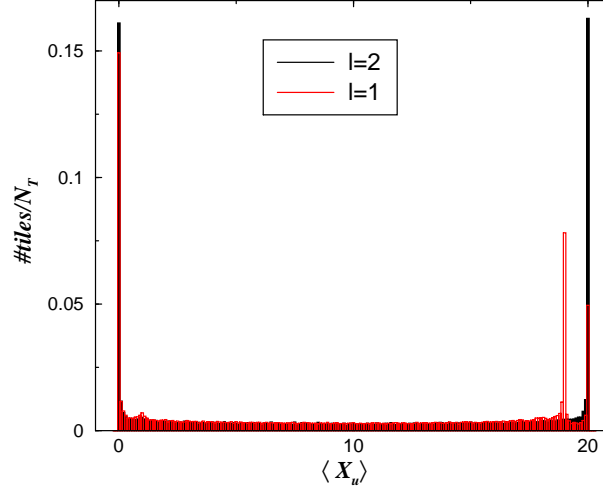


Figure 4.3: Parts distributions measured once tilings have reached stationarity or equilibrium. Here  $p = 20$ . We have represented two typical cases: icosahedral tilings (in red) and acyclic ones (in black). Besides the expected peaks at  $\langle X \rangle = 0$  and  $p$ , we observe additional peaks at  $\langle X \rangle = 1, 18$ , and  $19$  in the icosahedral case, which is the manifestation of ergodicity breaking.

One can see that these distributions are roughly speaking flat with two marked peaks at  $\langle X \rangle = 0$  and  $p$ , and an additional peak at  $\langle X \rangle = p - 1$  in the icosahedral case. The asymmetry of the distribution is essentially due to this anomalous peak. The two first peaks at  $\langle X \rangle = 0$  and  $p$  where expected because they are associated with the frozen regions near the boundary, which contains a macroscopic fraction of tiles. By contrast, the peak at  $p - 1$  reveals the existence of another large frozen region situated between the last and penultimate de Bruijn surfaces. In addition, two secondary peaks at  $\langle X \rangle = 1$  and  $18$  can be identified. They correspond to tiles situated between the first and second de Bruijn surfaces on the one hand, and the penultimate and antepenultimate ones on the other hand. In out-of-equilibrium tilings, such tiles are more numerous than expected.

These observations suggest that de Bruijn surfaces have difficulties to reach their equilibrium average positions in icosahedral tilings, in other words that they are pinned by some tiling “defects”. This observation does not concern only the most external de Bruijn surfaces, since the secondary peaks indicate that inner surfaces are also affected. Such peaks certainly exist for other values of  $\langle X \rangle$ , but statistical noise did not allow us to distinguish them from the “normal” flat distribution.

What are these defects that we have just invoked to account for the observed dynamical slowing down? It is tempting to attribute it to the previously mentioned cycles, because we



know that de Bruijn surfaces cannot go through them without a possibly long, preliminary cooperative tiling reorganization. Besides, we know that such cycles can have been created during the tiling evolution, because this phenomenon is also observed when the initial tiling  $T_0$  is acyclic. We do not need invoking unbreakable cycles to explain the slowing down. If a cycle has been created, it can be broken by reversing the evolution. An appealing hypothesis is that cycles could be entropically stabilized.

We have already mentioned that cycles are rare if  $p \lesssim 15$  and that slow dynamics have a few chance to be observed below this limit. For  $p = 10$ , we have not identified any slowing-down. By contrast, we have analyzed carefully the evolution of  $\Psi_{(a,T)}(t)$  for tilings of size  $p = 17$ . Indeed, it is reasonable to expect that equilibration time will not be extremely large just above the limit  $p \simeq 15$ , and that the unlocking of cycles (or other obstacles) will be observable. We have indeed observed such events at large times:  $\Psi_{(a,T)}$  stays around an out-of-equilibrium value and then jumps to another value, and so forth. This suggests that the system jumps from some local free energy minima to other ones by passing over entropy barriers. Their height is still reasonable at the time-scale of our simulations for  $p = 17$ . Unexpectedly, we have also observed that  $\Psi_{(a,T)}$  can wander around a value very close to  $p/2$ , the equilibrium value, before jumping to another value farther from  $p/2$ . Thus the stability of local minima is comparable to that of  $p/2$ .

## 5 Discussion

In this Paper, we have shown that even if the observed flip dynamics are in general consistent with the Langevin approximation that predicts equilibration time quadratic in the system size,  $p$ , this conclusion is erroneous for a few classes of edge orientations when  $D \geq 6$ , among which the icosahedral one of physical interest.

The classes where dynamics does not reach the expected equilibrium state coincide with those where it cannot be proven that the set of configurations,  $\mathcal{T}$ , is connected by flips. We proposed that the origin of flip dynamics comes from the existence of some robust obstacles to the movement of de Bruijn surfaces, the cycles, which are also the reason why the proof of connectivity fails. These obstacles exist at the length-scale of tiles and cannot be apprehended by the Langevin approach which relies on a coarse-grained representation of tilings.

Now we explain why the slowing down is not specific of the fixed-boundary tilings where it has been observed numerically, at least for  $D = 6$ . The reason why we chose tilings with such boundary conditions is that they are very easy to construct and to manipulate at the numerical level, in contrast with periodic-boundary ones [32]. The latter require the construction of approximants that are not even known for  $D = 7$ . In the case of icosahedral tilings, it has been already argued [7] that cycles can exist only in the central region,  $\mathcal{R}_{\text{free}}$ , which contains all the edge orientations, because the peripheral ones, that are

of effective  $5 \rightarrow 3$  type, are acyclic. Even though cycles were not the source of pinning, we know that the dynamics is rapid in  $5 \rightarrow 3$  tilings. Thus if dynamics is slowed down because de Bruijn surfaces are pinned, this pinning cannot occur in these peripheral regions and the slowing down is reminiscent of obstacles in the central region  $\mathcal{R}_{\text{free}}$ , which is equivalent to a free- or periodic-boundary tiling, as discussed in Section 2.3.

Whatever its exact nature, we have not been able to describe definitively the dynamical slowing down in terms of locking/unlocking of cycles. We have not been able to give a microscopic scenario, to estimate the times needed to jump over entropic barriers, or to precise whether we are dealing with a weak or strong ergodicity breaking. Since such slowing-down appears only for tilings exhibiting cycles whatever the leading vector  $e_a$ , we have naturally postulated that they constitute dynamical obstacles impeding surfaces movement. The present work is not definitive and a finer understanding of the subtle interplay between the cycles in the different de Bruijn families will be necessary in the future, in order to achieve a complete theory accounting for the observed ergodicity breaking.

What are the consequences of this dynamical slowing down? At the numerical level, the implications are dramatic. Monte Carlo simulations [14–19] explore icosahedral tiling sets by flips to extract some physical observables such as entropy, phasonic elastic constants or the couplings between phasons and phonons. But they are likely to be biased because they do explore only a small subset of the configuration set. These studies will have to be revisited at the light of our results. Note that even though the existence of slow (or glassy) dynamics was questioned in some of these references, they were never observed. We believe that, because of the absence of an absolute reference to assess the return to equilibrium – our  $p/2$  –, the time constants that were measured corresponded to the rapid modes, which indeed grow like  $p^2$ . In addition, simulations were certainly not long enough to observe the slowest modes exhibited by our work.

As far as the physical properties of quasi-crystals are concerned, it would be tempting to question the effects of slow dynamics on growth processes or dislocation mobility. However, we believe that it would be premature to draw any definitive conclusion on the basis of our sole work at the tile scale, without taking into account their atomic decoration. Indeed, as it was discussed for example in Ref. [26], even if tiles are robust entities with high cohesion energies, they are not unbreakable, and it can be favorable for the system to break such structures to avoid an excessive cost, either energetic or entropic. Obstacles such as cycles could be bypassed by temporarily breaking tiles in order to allow the de Bruijn surfaces to cross them. Nevertheless, as far as diffusive properties are concerned, it has been shown [7] that these obstacles do not affect the diffusion of vertices. This conclusion is important because flip-assisted self-diffusion is believed to be an important and original property of quasi-crystalline alloys.

Finally, it should be emphasized that the present study does not involve energy. In other words, it is performed in the large temperature limit. Inter-atomic interactions can be taken

into account, in good approximation, by an effective Hamiltonian at the tile level [6,17–19]. Its introduction will certainly complicate any analytical work but we believe that, at the simulation level, slowness will survive at finite temperature, because cycles are geometric structures that exist whatever the tile interactions.

## References

- [1] D. Shechtman, I. Blech, D. Gratias, J.W. Cahn, Metallic Phase with Long-Range Orientational Order and No Translational Symmetry, *Phys. Rev. Lett.* **53**, 1951 (1984).
- [2] V. Elser, Comment on “Quasicrystals: a New Class of Ordered Structures”, *Phys. Rev. Lett.* **54**, 1730 (1985).
- [3] G. Coddens, C. Soustelle, R. Bellissent, Y. Calverac, Study of hopping in perfect icosahedral AlFeCu quasi-crystal by inelastic neutron scattering, *Europhys. Lett.* **23**, 33 (1993).
- [4] S. Lyonnard, G. Coddens, Y. Calvayrac, D. Gratias, Atomic (phason) hopping in perfect icosahedral quasicrystals  $\text{Al}_{70.3} \text{Pd}_{21.4} \text{Mn}_{8.3}$  by time-of-flight quasielastic neutron scattering, *Phys. Rev. B* **53**, 3150 (1996).
- [5] K. Edagawa, K. Suzuki, S. Takeuchi, High resolution transmission electron microscopy observation of thermally fluctuating phasons in decagonal Al-Cu-Co, *Phys. Rev. Lett.* **85**, 1674 (2000).
- [6] M. Mihalkovic, et al., Total-energy-based prediction of a quasicrystal structure, *Phys. Rev. B* **65**, 104205 (2002).
- [7] V. Desoutter, N. Destainville, Flip dynamics in three-dimensional random tilings, *J. Phys. A: Math. Gen.* **38**, 17 (2005).
- [8] L. Leuzzi, G. Parisi, Thermodynamics of a tiling model, *J. Phys. A: Math. Gen.* **33**, 4215 (2000).
- [9] C. Castelnovo, P. Pujol, C. Chamon, Dynamical obstruction in a constrained system and its realization in lattices of superconducting devices, *Phys. Rev. E* **69**, 104529 (2004).
- [10] U. Grimm, D. Joseph, Modelling quasicrystal growth, in *Quasicrystals - An introduction to structure, physical properties and applications*, J.-B. Suck, M. Schreiber, P. Häussler, 199 (Springer, 2002).
- [11] P.A. Kalugin, A. Katz, A mechanism for self-diffusion in quasi-crystals, *Europhys. Lett.* **21**, 921 (1993).
- [12] M. Wollgarten, M. Beyss, K. Urban, H. Liebertz, U. Köster, Direct evidence for plastic deformation of quasicrystals by means of a dislocation mechanism, *Phys. rev. Lett.* **71**, 549 (1993).
- [13] K. Urban, M. Feuerbacher, M. Wollgarten, M. Bartsch, U. Messerschmidt, in *Physical Properties of Quasicrystals*, Ed. Z.M. Stadnik, *Solid State Science* **126**, Springer, 361 (1999).

- [14] L.-H. Tang, Random-tiling Quasicrystals in Three Dimensions, *Phys. Rev. Lett.* **64**, 2390 (1990).
- [15] L.J. Shaw, V. Elser, C.L. Henley, Long-range order in a three-dimensional random-tiling quasicrystal, *Phys. Rev. B* **43**, 3423 (1991).
- [16] K.J. Strandburg, Entropy of a three-dimensional random-tiling quasicrystal, *Phys. Rev. B* **44**, 4644 (1991).
- [17] T. Dotera, P.J. Steinhardt, Ising-like transition and phason unlocking in icosahedral quasicrystals, *Phys. Rev. Lett.* **72**, 1670 (1994).
- [18] F. Gähler, Thermodynamics of random tiling quasicrystals, in *Proceedings of the 5th International Conference on Quasicrystals (ICQ5)*, Eds. C. Janot, R. Mosseri (World Scientific, 1995).
- [19] W. Ebinger, J. Roth, H.-R. Trebin, Properties of random tilings in three dimensions, *Phys. Rev. B* **58**, 8338 (1998).
- [20] C.L. Henley, Random Tiling Models, in *Quasicrystals, the State of the Art*, Eds. D.P. Di Vincenzo, P.J. Steinhardt (World Scientific, 1991), 429.
- [21] N.G. de Bruijn, Algebraic theory of Penrose's non-periodic tilings of the plane, *Kon. Nederl. Akad. Wetensch. Proc. Ser. A* **84**, 1 (1981).
- [22] N.G. de Bruijn, Dualization of multigrids, *J. Phys. France* **47**, C3-9 (1986).
- [23] D. Randall, P. Tetali, Analyzing Glauber dynamics by comparison of Markov chains, *J. Math. Phys.* **41**, 1598 (2000).
- [24] N. Destainville, Flip dynamics in octagonal rhombus tiling sets, *Phys. Rev. Lett.* **88**, 030601 (2002).
- [25] J. Linde, C. Moore, M.G. Nordahl, An  $n$ -dimensional generalization of the rhombus tilings, in *Proceedings of the Conference DM-CCG: Discrete Models: Combinatorics, Computation, and Geometry* (Paris, 2001), p. 23.
- [26] M. Widom, R. Mosseri, N. Destainville, F. Bailly, Arctic octahedron in three-dimensional rhombus tilings and related integer solid partitions, *J. Stat. Phys.* **109**, 945 (2002).
- [27] H. Cohn, R. Kenyon, J. Propp, A variational principle for domino tilings, *J. Amer. Math. Soc.* **14**, 297 (2001).
- [28] N. Destainville, Entropy and boundary conditions in random rhombus tilings, *J. Phys. A: Math. Gen.* **31**, 6123 (1998).
- [29] G.D. Bailey, *Tilings of zonotopes: Discriminantal arrangements, oriented matroids, and enumeration*, Ph. D. Thesis (Univ. of Minnesota, 1997).
- [30] V. Desoutter, *Etude de deux systèmes dynamiques dominés par des phénomènes entropiques*, Ph. D. Thesis (Univ. Toulouse 3, 2005).
- [31] R. Zwanzig, *Nonequilibrium statistical mechanics* (Oxford University Press, 2001).
- [32] M.V. Jarić, E. Sørensen, Self-diffusion in random-tiling quasicrystals, *Phys. Rev. Lett.* **73**, 2464 (1994).